Available online at www.sciencedirect.com
ScienceDirect
Mendeleev Commun., 2008, **18**, 128–130
Mendeleev Communications

Density functional theoretical study of the electronic structure and vibrational spectra of a polynuclear $[Mg_2(MeOH)_4Mo_8O_{22}(OMe)_6]^{2-}$ complex

Tatyana A. Savinykh*, Alexander F. Shestakov, Nadezhda V. Bardina, Tamara A. Bazhenova and Yurii M. Shulga

Institute of Problems of Chemical Physics, Russian Academy of Sciences, 142432 Chernogolovka, Moscow Region, Russian Federation. Fax: +7 496 515 5420; e-mail: tfil@icp.ac.ru

DOI: 10.1016/j.mencom.2008.05.005

The molecular and electronic structures and the vibrational spectra of the mixed-valence Mg–Mo cluster $[Mg_2(MeOH)_4Mo_4^{VI}Mo_4^{V}O_{22}(OMe)_6]^{2-}$ were calculated to locate two pairs of Mo^V centers with strong Mo–Mo bonding.

Biological nitrogen fixation by nitrogenase is an important naturally occurring process. Functional chemical models of this enzyme are known. They contain polynuclear heterometallic complexes, which, probably, are capable of the multicenter binding of the dinitrogen molecule with its selective activation to following reduction reactions.[1] Polynuclear Mo^{III} containing clusters catalysing dinitrogen reduction under conditions resembling biological ones with rates typical of nitrogenase are of special interest. At the same time, the active center of nitrogenase, a Fe–Mo cofactor, in the isolated form is capable of only reversible N_2 molecule binding.[2,3] Therefore, to understand the role of the surroundings, information on the structure of the synthetic active center is of special importance.[3] However, the experimental determination of its structure is difficult to perform. Only the structure of a catalyst precursor, mixed-valence cluster $[Mg_2(MeOH)_4Mo_4^{VI}Mo_4^{V}O_8(\mu_2\text{-}O)_8(\mu_2\text{-}OMe)_6(\mu_3\text{-}O)_4(\mu_4\text{-}O)_2]^{2-}$ **1** is known.[4]

It is reasonable to use theoretical modeling for understanding the structure of **1** in the reduced state. Here, we report the results of calculations by density functional methods for the electronic structure and arrangement of initial complex **1**.

The complex $[Mg_2Mo_8O_{22}(MeO)_6(MeOH)_4]^{2-}[Mg(MeOH)_6]^{2+}\cdot 6MeOH$ was synthesised as described previously.[4] The calculations were carried out by the B3LYP density functional method using the LANL2DZ basis set implemented in the Gaussian 03 program package (Revision C.02).[5] Alternative calculations by the PBE density functional method[6] using extended basis sets Mo[5*s*5*p*3*d*], Mg[2*s*2*p*], C,O[3*s*3*p*2*d*] and H[3*s*1*p*] for SBK pseudopotential[7] implemented in the Priroda program package[7] were also performed. The IR spectra of complex **1** in KBr pellets were recorded on a Perkin-Elmer Spectrum BX2 Fourier transform spectrometer within the region 400–4000 cm^{-1} with a spectral resolution of 2 cm^{-1}. The IR spectrum of complex **1** in Nujol was measured on a Bruker IFS-66S IR Fourier transform spectrometer. The Raman spectrum of the complex was recorded on a Nicolett 9810 Fourier spectrometer (λ = 976 nm).

An unusual feature of the cluster structure is an irregular arrangement of four bridge OMe groups at Mo atoms: the coordination sphere of two of eight Mo atoms does not contain these groups at all [Figure 1(*a*)]. The calculations show that the isomer complexes with more regular allocation of bridge methoxy groups [Figure 1(*b*),(*c*)] have energies 1.1 and 2.3 kcal mol^{-1} higher, respectively, according to PBE/SBK calculations. The geometry of the main isomer is in agreement with the X-ray analysis data.[1] The root-mean-square deviations in bond lengths and angles are 0.12 Å and 3.15° for B3LYP method and 0.10 Å and 2.71° for PBE method. The theoretical bond lengths, as a rule, are greater than experimental ones.

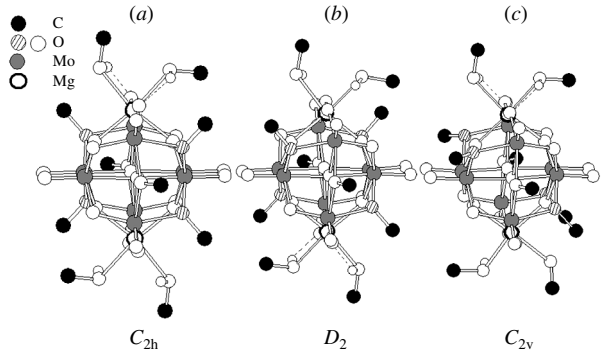

Figure 1 Structures of isomeric Mo_8Mg_2 complexes. O atoms, shown as dashed circles, belong to bridging methoxy groups. H atoms are omitted for clarity.

Four Mo centers in the structure are in two pairs with short distances of 2.645 and 2.660 Å, for B3LYP and PBE functionals, respectively; the experimental value is 2.587 Å.[1] The lengths of bridging Mo–μ_2-O bonds make up 1.821 and 1.824 Å (PBE); the experimental values are 1.749 and 1.746 Å.[1] The Mg–μ_2-O distances are equal to 2.033 and 2.039 Å (PBE), the experimental values 1.983 and 2.009 Å. The maximal discrepancy is observed for terminal Mg–O bond lengths, which are longer than experimental ones by 0.23 (B3LYP) and 0.26 Å (PBE). The reason of the noticeable bond shortening, in our opinion, consists in the high polarity and modest force constants for the donor–acceptor bonds $Mg^{2+}\leftarrow O(Me)H$.

For the main isomer (C_{2h}), various spin states have been considered. The complex in the singlet state has the lowest energy. At the geometry relaxation the energies of excited states with $S = 1$ and $S = 2$ noticeably decrease. The spin and charge density distributions, as well as the relative energies for various spin states, are presented in Table 1. In the mixed-valence cluster, there are two shortened Mo–Mo distances. Spin density for excited triplet and quintet states is presumably located just on these centers (Table 1) and consecutive Mo–Mo bond cleavage with an increase in Mo–Mo distances from 2.65 to 3.0 Å occurs under geometry relaxation. Adiabatic energies of singlet-triplet

Table 1 Spin and charge density distributions and relative energies of the initial $[Mg_2(MeOH)_4Mo_8O_{22}(OMe)_6]^{2-}$ and model $[Mg_2(HOH)_4Mo_8O_{22}(OH)_6]^{2-}$ complexes in various spin states (PBE data).

Spin	Model complex	Initial complex					
	Relative energy/ kcal mol^{-1}		Spin density, spin of electron			Charge, abs. value of charge of electron		
			Mo[a]	Mo[b]	Mo[c]	Mo[a]	Mo[b]	Mo[c]
$S = 0$	0	0	0.00	0.00	0.00	2.43	2.43	2.43
$S = 1$	45.5	40.5	0.05	0.00	0.92	0.59	2.43	2.49
	14.7[d]	15.6[d]	0.07[d]	0.01[d]	0.77[d]	2.43[d]	2.43[d]	2.44[d]
$S = 2$	90.9	81.1	0.09	0.91	0.91	2.43	2.48	2.48
	30.3[d]	30.8[d]	0.14[d]	0.78[d]	0.78[d]	2.42[d]	2.44[d]	2.66[d]

[a]Atoms do not form Mo–Mo bond. [b]Atoms of the first breaking Mo–Mo bond. [c]Atoms of the second breaking Mo–Mo bond. [d]The values correspond to the adiabatic spin uncoupling.

and triplet-quintet transitions coincide with high accuracy: 15.4±0.2 kcal mol^{-1}. This value represents a rough estimate of the Mo–Mo bond energy. The above data suggest that the reason for the formation of a shortened Mo–Mo bond is the presence of *d*-electrons at the metal atoms.

On this basis, an important conclusion can be drawn. In the reduced active state of the cluster, which is reached when 20 electrons are transferred on it, all Mo atoms become trivalent and get an electronic configuration of d^3. In view of strong interactions between the Mo centers having *d* electrons, it is possible to expect the appearance of up to 10 new Mo–Mo bonds in the reduced cluster, and, thus, essential reorganization of its metal frame. In principle, this allows us to assume the arising of conditions for the formation of binuclear complexes with dinitrogen, the most effective for N–N bond activation.

For the basic structure the geometry change under replacement of all OMe ligands by OH groups is investigated. The framework of the structure of this model complex differs a little in geometry from the initial one. The lengths of Mo–Mo and Mo–μ_4-O bonds are practically unchangeable and only a small decrease in Mo–μ_2-O bond lengths on 0.01–0.03 Å occurred. The relative energies of excited states for the model and initial complexes are consistent. The removal of two H_2O molecules from the coordination sphere of Mg atoms in the model complex requires an unusually small energy consumption of 11.7 kcal mol^{-1}. The reason is in strengthening the interaction of Mg ions with the internal μ_4-O atom. The calculations show that, for related $[Mo^{VI}O_2Mg(MeOH)_2(OMe)_4]_2$ clusters[4] with a similar coordination environment of Mg ions but without internal μ_4-O atom, the binding energy of water molecules was approximately twice as large.[9]

Theoretical IR and Raman spectra of the complex (Figure 2) are constructed on the basis of calculated frequencies and intensities with the Lorentz smoothing of the lines of 10 and 20 cm^{-1}, respectively, which exceeds the experimental spectral resolution but corresponds to the half-width of single lines. The structure of the calculated and experimental IR spectra has a certain similarity that gives the basis for the assignment of lines, the sequence of the certain types of vibrations upon increase of the wave number and divergences between two calculated spectra being taken into account. In further discussions, the values are grouped in such a way that the positions of corresponding experimental lines go first; then (in parentheses), the PBE data, if they are available, and the B3LYP data. The assignment of vibrations in the region 100–400 cm^{-1}, where number and position bands in IR and Raman spectra differ noticeably, is difficult to perform.

The Mo^{VI}–μ_4-O stretching vibrations give a weak absorption band at (426, 455) 438, 462 cm^{-1} in the theoretical IR spectrum

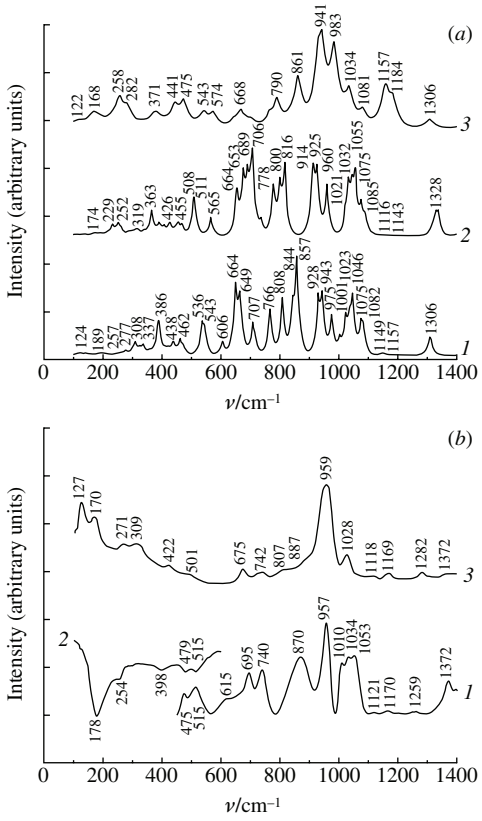

Figure 2 (*a*) Theoretical IR spectra: (*1*) B3LYP/LANL2DZ, (*2*) PBE/SBK, and (*3*) Raman spectra, B3LYP/LANL2DZ of the $[Mg_2(MeOH)_4Mo_8O_{22}(OMe)_6]^{2-}$ complex; (*b*) vibrational spectra of $[Mg_2Mo_8O_{22}(MeO)_6(MeOH)_4]^{2-}[Mg(MeOH)_6]^{2+}\cdot 6MeOH$ complex: (*1*) IR in KBr, (*2*) IR in Nujol and (*3*) Raman spectra.

and do not appear in the experimental IR spectrum. According to calculation, their intensity increase in Raman spectrum, which determine the appearance of the peak at 422 (441, 475) cm^{-1}. Stretching Mo^V–μ_4-O vibrations are observed in both IR at 475, 515 (508, 511) 536, 543 cm^{-1} and Raman spectrum at 501 (543, 574) cm^{-1}. The Mo–μ_2-O(Me) stretching vibrations manifest themselves as a band at 615 (565) 606 cm^{-1} only in the IR spectrum. Next bands in the IR spectrum, 695 (653, 664) 649, 664 cm^{-1} and 740 (689, 706) 707, 766 cm^{-1}, correspond to anti-phase and in-phase mode of H–O–Mg stretching vibrations and Mg–μ_3-O stretching vibrations, respectively. In the Raman spectrum, these vibrations appear at 675 and 742 cm^{-1}, respectively, and form a wide absorption band at 668 cm^{-1} in the theoretical Raman spectrum. The stretching Mo-μ_2-O(Mo) vibrations [870 (778) 808 cm^{-1}] and Mo-μ_2-O(Mg) vibrations [870 (800, 816) 844, 857 cm^{-1}], correspond to a wide absorption band in the IR spectrum but give two individual bands at 807 (790) and 887 (861) cm^{-1} in the Raman spectrum. The intense peak in the IR spectrum at 870 (914, 925, 960) 928, 943, 975 cm^{-1} or the one at 959 (941 and 983) cm^{-1} in the Raman spectrum correspond to unresolved in-phase and anti-phase modes of Mo^V=O and Mo^{VI}=O stretching vibrations, respectively.

The wide group of absorption bands in the IR spectrum is connected with different C–O vibrations of methoxy ligands: 1010 (1021) 1001 cm^{-1} with stretching C–O(Mo) vibrations, 1034 (1032) 1023 cm^{-1} with stretching in-phase C–μ_2-O(Mg) vibrations, and 1053 (1055, 1075, 1085) 1046, 1075, 1088 cm^{-1} with stretching C–μ_2-O(Mo) vibrations. In the Raman spectrum, only C–O vibrations of methoxy groups are observed at 1028 (1034, 1081) cm^{-1}. The overlying absorption bands at 1121 (1116) 1149; 1170 (1143) 1157; 1372 (1328) 1306 and 1456 (1424) 1510 cm^{-1} in the IR spectrum and 1118 (1157); 1169 (1184);

1372 (1306) and 1449 (1465) cm^{-1} in the Raman spectrum correspond to the bending vibrations of the methyl group and the H–O–C bending vibrations of MeOH ligands.

We are grateful to A. I. Karelin for the recording of the IR spectrum in the low-frequency region.

References

1 M. Yu. Antipin, L. P. Didenko, L. M. Kachapina, A. E. Shilov, A. K. Shilova and Yu. T. Struchkov, *J. Chem. Soc., Chem. Commun*., 1989, 1467.
2 T. A. Bazhenova, M. A. Bazhenova, G. N. Petrova and S. A. Mironova, *Kinet. Katal.*, 2002, **43**, 592 [*Kinet. Catal*. (*Engl. Transl.*), 2002, **43**, 219].
3 N. V. Bardina, T. A. Bazhenova, G. N. Petrova, A. K. Shilova and A. E. Shilov, *Izv. Akad. Nauk, Ser. Khim.*, 2006, 766 (*Russ. Chem. Bull., Int. Ed*., 2006, **55**, 793).
4 M. Yu. Antipin, Yu. T. Struchkov, A. E. Shilov and A. K. Shilova, *Gazz. Chim. Ital*., 1993, **123**, 256.
5 M. J. Frisch, G. W. Trucks, H. B. Schlegel, G. E. Scuseria, M. A. Robb, J. R. Cheeseman, J. A. Montgomery, Jr., T. Vreven, K. N. Kudin, J. C. Burant, J. M. Millam, S. S. Iyengar, J. Tomasi, V. Barone, B. Mennucci, M. Cossi, G. Scalmani, N. Rega, G. A. Petersson, H. Nakatsuji, M. Hada, M. Ehara, K. Toyota, R. Fukuda, J. Hasegawa, M. Ishida, T. Nakajima, Y. Honda, O. Kitao, H. Nakai, M. Klene, X. Li, J. E. Knox, H. P. Hratchian, J. B. Cross, C. Adamo, J. Jaramillo, R. Gomperts, R. E. Stratmann, O. Yazyev, A. J. Austin, R. Cammi, C. Pomelli, J. W. Ochterski, P. Y. Ayala, K. Morokuma, G. A. Voth, P. Salvador, J. J. Dannenberg, V. G. Zakrzewski, S. Dapprich, A. D. Daniels, M. C. Strain, O. Farkas, D. K. Malick, A. D. Rabuck, K. Raghavachari, J. B. Foresman, J. V. Ortiz, Q. Cui, A. G. Baboul, S. Clifford, J. Cioslowski, B. B. Stefanov, G. Liu, A. Liashenko, P. Piskorz, I. Komaromi, R. L. Martin, D. J. Fox, T. Keith, M. A. Al-Laham, C. Y. Peng, A. Nanayakkara, M. Challacombe, P. M. W. Gill, B. Johnson, W. Chen, M. W. Wong, C. Gonzalez and J. A. Pople, *Gaussian 03, Revision C.02*, Gaussian, Inc., Wallingford CT, 2004.
6 J. P. Perdew, K. Burke and M. Ernzerhof, *Phys. Rev. Lett.*, 1996, **77**, 3865.
7 W. J. Stevens, H. Basch and M. J. Krauss, *Chem. Phys*., 1984, **81**, 6026.
8 D. N. Laikov, *Chem. Phys. Lett*., 1997, **281**, 151.
9 T. A. Savinykh and A. F. Shestakov, *Izv. Akad. Nauk, Ser. Khim*., 2008, 441 (in Russian).

Received: 4th September 2007; Com. 07/3005